RSC Advances

ROYAL SOCIETY OF CHEMISTRY

www.rsc.org/advances

Complexing Agent Study for Environmentally Friendly Silver Electrodeposition (Ⅱ): Electrochemical Behavior of Silver-Complex

Anmin Liu, Xuefeng Ren, Jie Zhang, Deyu Li, and Maozhong An*

State Key Laboratory of Urban Water Resource and Environment, School of Chemical Engineering and Technology, Harbin Institute of Technology, Harbin, 150001, China.

** Correspondence to:*

mzan@hit.edu.cn (Maozhong An), Tel/ Fax: +86-451-86418616

Abstract:

Electrochemical behaviors of silver-complex in the environmentally friendly silver plating bath with 5,5-Dimethylhydantoin (DMH) and Nicotinic acid (NA) as complexing agents were investigated in this paper. Equally to the cyanide based silver electroplating bath, silver deposits with smooth and compact morphologies, as well as high purity could be obtained from the studied DMH and NA based silver electroplating bath. The electrochemical behaviors of silver-complex in this cyanide-free silver electroplating were studied by cyclic voltammetry with different sweep rate to investigate the discharge process of the silver plating bath, the transfer coefficients and diffusion coefficient of silver-complex in this bath were studied. The results of the chronoamperometry on the glass carbon electrode indicate that the nucleation processes of silver from the bath is three-dimensional progressive nucleation process, and the growth of silver nucleation and the nucleation rate of silver deposit in DMH and NA based silver plating bath were highly depended on the applied potential.

1. Introduction

Silver deposit is widely applied in many industrial areas owe to its excellent physical and chemical properties.[1-4] Electrodeposition is one of the most important and low cost methods to get excellent silver deposit for variety of applications, in which, the cyanide based electroplating baths were used for more than 100 years to obtain compact, smooth, and adhesive silver deposits with the most consistent quality at the lowest cost.[5-9] Unfavorably, as one of the most poisonous chemicals, cyanide brings extremely high hazardous risks to human health and the environment.[10] Furthermore, with the increasing pressure of environmental protection, the disposal of exhausted electroplating baths and waste water are becoming more and more difficult and expensive.[11, 12]

In order to overcome these challenges and eliminate cyanide based baths, a number of attempts have been made in past few years to develop cyanide-free silver electroplating baths. Among them, the complexing agents for cyanide-free silver electroplating were widely investigated owing to its important roles during the electroplating process. Complexing agents for cyanide-free silver electroplating baths, such as thiosulfate[13-16], uracil,[17] ammonia,[18, 19] sodium citrate[20], HEDTA,[21] 2-hydroxypyridine,[22, 23] and ionic liquids[10, 24] have been proposed. Nevertheless, except for few successful cases, most of these baths still suffer from problems of instability of electroplating baths and low deposit quality, including sever adhesion and inferior morphologies. Consequently, more efforts should be directed toward this area to find a comparable and environmental friendly alternative to cyanide based silver electroplating baths.

5,5-dimethylhydantoin (DMH) and nicotinic acid (NA), two heterocyclic structure organics, were selected as complexing agents for cyanide-free silver

electroplating in our study.[25, 26] Compared to other reported complexing agents used for cyanide-free silver electroplating baths, the DMH and NA molecules with good solubility and stability in alkaline solution in a large temperature range, act as more stable complexing agents for silver(I).[27] In order to improve the practicability of the introduced bath and silver deposit in more and more areas, a variety of DMH and NA based cyanide-free silver electroplating baths were developed.[25, 26, 28]

Besides the application of silver deposits in electronics or other industry, the investigation of electrochemical behaviors of silver-complex in the environmental friendly silver plating bath is of great importance. The cathodic deposition process [29-31] and the nucleation and growth mechanism[22, 32-36] were the most important properties to study the electrochemical behaviors of silver-complex in the DMH and NA based cyanide-free silver plating baths.

In the present work the performances of the silver deposit obtained from the DMH and NA based silver electroplating bath were determined by experiments and compared with that from the cyanide based bath. As equal to the cyanide based silver electroplating bath, a mirror bright silver deposit, with excellent leveling capability, smooth and compact morphologies, and high purity could be obtained from the studied DMH and NA based silver electroplating bath. The cathodic deposition process of silver-complex in the investigated cyanide-free silver electroplating bath was investigated by cyclic voltammetry. Chronoamperometry was employed to explore the initial process of the silver electrodepostion, including the nucleation growth and mechanism. Cathodic polarization was demonstrated by potentiodynamic cathodic polarization curves on the Pt rotating disk electrode to study the activation energy of the silver electrodeposition process.

2. Experimental

All silver electroplating baths used in this work were prepared using analytical grade reagents and deionized water. The introduced silver electroplating bath was prepared by adding 0.075 M $AgNO_3$ solution into a electrolyte containing 0.7 M DMH, 0.7 M NA, and 1.3 M K_2CO_3, the pH value of the electroplating bath was adjusted to 10.0~14.0 with KOH solution after the addition of $AgNO_3$ solution. Silver electroplating experiments were conducted under galvanostatic conditions (at 0.8 A dm^{-2}) in a cell employing the copper sheet as the cathodic substrate.

Field emission scanning electron microscopy (FE-SEM) was employed to characterize the surface morphologies of the silver deposits obtained from the introduced silver electroplating bath and the cyanide based one. The investigation of impurities in these two studied silver deposits was performed by Auger Electron Spectroscopy (AES), the original surface and a 1.0 nm depth of silver deposit were studied to analyze the contents of Ag, C, N, and O to investigate the impurity in the silver deposits from the introduced electroplating bath and cyanide based electroplating bath.

All electrochemical measurements were performed in a typical three-electrode cell connected with an electrochemical workstation. A platinum foil and a mercuric oxide electrode (Hg/HgO) were employed as the counter electrode (CE) and the reference electrode (RE), respectively. A glassy carbon electrode (GCE) with a diameter of 3 mm was used for cyclic voltammetry (CV) and chronoamperometry (I-t) measurements.

3. Results and discussion

3.1 Morphology of silver deposits

The surface morphology is a very important consideration for most of the silver

deposit applications. Fig. 1 displays the top view SEM images of the silver deposits obtained from cyanide based electroplating bath and the cyanide-free electroplating bath introduced in this work.

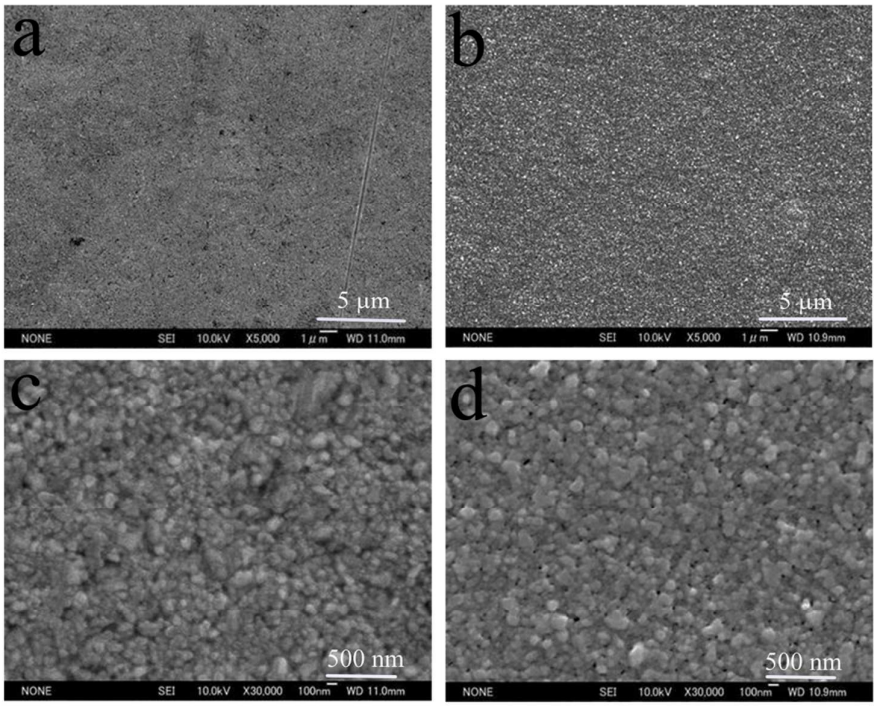

Fig. 1 Top view SEM images of full bright silver deposits obtained from different silver electroplating baths, (a) and (c) from the cyanide based silver electroplating bath, (b) and (d) from the DMH and NA based silver electroplating bath.

From the comparison of the low definition images (Fig. 1 (a) and 1 (b)), the silver deposits obtain from the two baths has the same flatness. On the other hand, no difference can be observed between the high definition images (Fig. 1 (c) and 1 (d)), as the grain size and compactness are also same. Therefore, the silver deposits from these two electroplating baths have the same morphology. It can therefore be concluded that mirror bright silver deposits on copper substrates, with excellent leveling capability, smooth and compact morphologies as well as tiny silver particles, can be obtained from the investigated DMH and NA based cyanide-free silver electroplating bath.

3.2 Purity of silver deposit

Impurity, the interfused organic complexing agents or additives in the deposits, is another key consideration in silver electrodeposition, because it seriously affects the properties and quality of the resulting silver deposits. When applied in microelectronics or decorative industries, the vitally important anti-tarnish abilities and electrical properties of the silver deposits are severely compromised by the interfused impurities.[37-39] In order to investigate the impurity in the silver deposits from the DMH and NA based electroplating bath, comparing with that from cyanide based electroplating bath, AES analysis was carried out to examine the composition and proportion of the atoms in the silver deposits.

Fig. 2 displays the composition of the original surface and a 1.0 nm depth of silver deposit obtained from the introduced cyanide-free electroplating bath and the cyanide one. The proportion of atoms at the original surface and a 1.0 nm depth of silver deposit measured by AES are shown in Table 1.

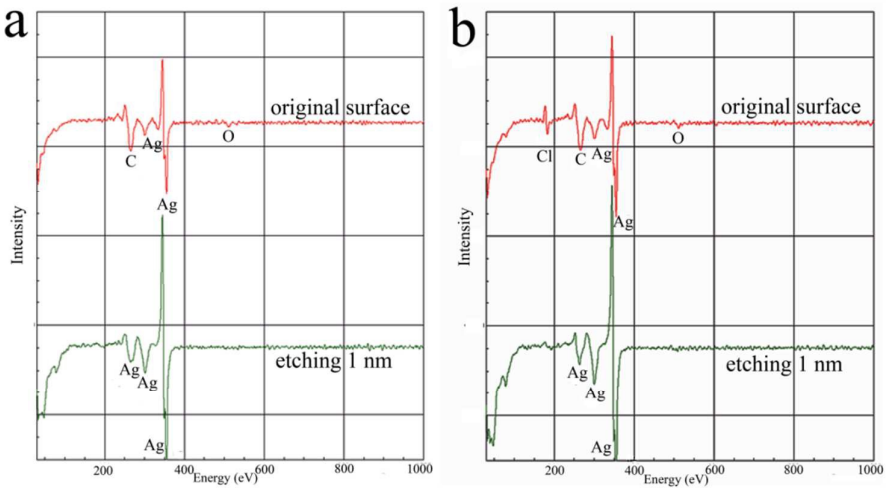

Fig. 2 AES spectra of the original surface and a 1.0 nm depth of silver deposits, (a) from the cyanide based silver electroplating bath, (b) from the DMH and NA based silver electroplating bath.

As displayed in Fig. 2 (a), Ag, C, N, and O were present on the original surface

of deposit from cyanide based silver electroplating bath. Contrastingly, besides the signals of Ag, C, N, and O, signal for Cl could be detected on the original surface of deposit from the introduced cyanide-free silver electroplating bath as shown in Fig. 2 (b). But signal for Cl could not stand for the contaminant on silver surface as no Cl was used in the bath and it was only in the top 1.0 nm.

Table 1 Concentration of atoms at the original surface and a 1.0 nm depth of silver deposit measured by AES. (Unit of Atom %)

		Ag	C	O	Cl
Cyanide deposit	original surface	31.1	64.6	4.3	0
	etching 1 nm	100.0	0	0	0
Cyanide-free deposit	original surface	37.2	52.4	4.4	6.0
	etching 1 nm	100.0	0	0	0

On the other hand, no signals for C, N, O, and Cl could be detected at the 1.0 nm depth of silver deposit in the sensitivity limit of AES, indicating that all these organic impurities only adsorbed on the surface of cyanide and cyanide-free based silver deposits, and the purity of the silver deposit was very high.

With high purity, the introduced cyanide-free silver deposit could own excellent anti-tarnish abilities and electrical properties. Surface adsorption of organic impurities could not influence the conductivity of the bulk silver since the surface adsorption layer was only a single molecular layer. Thus, the silver deposit obtained from the introduced bath could be used in microelectronics and decorative applications due to its high purity, excellent anti-tarnish abilities and electrical properties.

3.3 Study of discharge process

The cathodic discharge process of silver-complex in the investigated cyanide-free silver electroplating bath was investigated by cyclic voltammetry (CV).

The potential scan started at the open circuit potential (OCP) toward the negative direction with a sweep rate of 20 mV s^{-1} from -1.35 V to 1.10 V, as shown in Fig. 3.

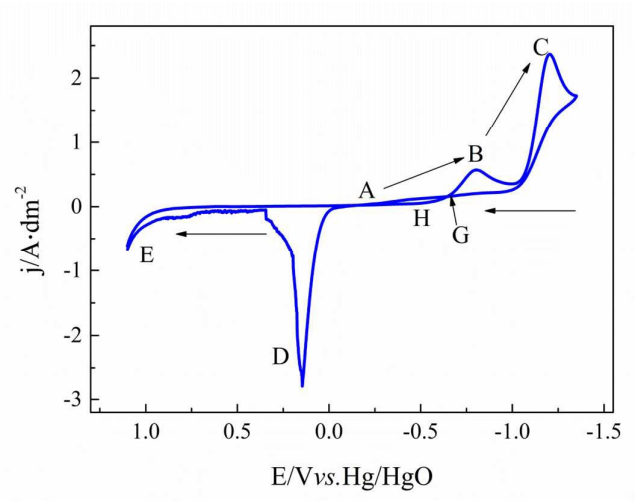

Fig. 3 Cyclic voltammograms with a sweep rate of 20 mV s^{-1} on the GCE of the investigated silver electroplating bath.

In the forward scan, with the scanning potential reaches a relatively negative value (at point H) the cathodic current begins increasing and results in a cathodic peak (at point B), then the cathodic current decreases with the scanning potential reaches more negative for the diffusion control until the current increase of hydrogen evolution area (at point C). In the positive direction scanning, the cathodic current decreases slowly and makes the reverse curve intersect the forward cathodic current curve at point G, resulting in forming a "hysteresis loop", a characteristic of the three-dimensional (3D) nucleation and growth of silver on the GCE surface.[40-43] In addition, an anodic dissolution peak of silver deposit (at point D) and an oxygen evolution area (at point E) emerged during the positive direction scanning.

CVs displayed in Fig. 4 at various sweep rates on 3 mm GCE were performed to study the electrochemical behaviors of silver-complex in the cathodic deposition process, including the control step of silver electrodeposition, the transfer coefficient, and the diffusion coefficient.

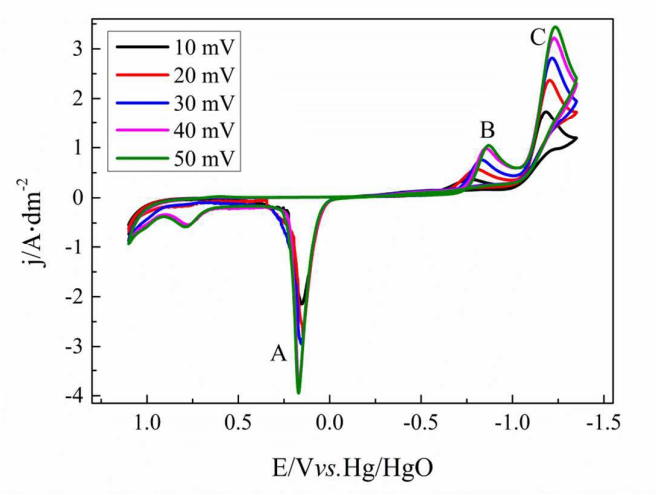

Fig. 4 Cyclic voltammograms with different sweep rates on the GCE of the studied silver electroplating bath.

As displayed in Fig. 4, the cathodic peak (B) current density j_p was different with the anodic peak (A) current density, it increases with the increase of the sweep rate and the cathodic peak (B) potential (E_p) moved to more negative side as the sweep rate increased. These results indicate that the deposition process of silver-complex in the DMH and NA based bath is irreversible.

For the irreversible cathodic electrode process, following equations can be used to study the kinetic features of the silver deposition process.[44]

$$\left|E_p - E_{p/2}\right| = 1.857RT/(\alpha nF) \quad (1)$$

$$j_p = 0.4958(nF)^{3/2}(\alpha Dv)^{1/2}(RT)^{-1/2}c \quad (2)$$

Where E_p is the peak potential, $E_{p/2}$ is the potential at half of the peak current density, j_p is the cathodic peak current density, n is the number of electrons involved in the silver electro deposition reaction (n = 1), F is the Faraday constant, α is the charge transfer coefficient, D is the diffusion coefficient, v is the scan rate, R is gas constant, T is temperature (T = 328 K), and c is the concentration of electroactive species in the bath (c = 0.075 M). The transfer coefficients (α) of Ag-complex in the studied bath

can be calculated using Eq. (1) from CV curves in Fig. 4, as displayed in Table 2. Thus, the average transfer coefficient was calculated as 0.615 in the silver plating bath containing 0.075 M Ag-complex.

Table 2 The transfer coefficients (α) calculated from CV curves at various scan rates on GCE.

v / mV s^{-1}	j_p / A dm^{-2}	E_p / V	$\mid E_p$-$E_{p/2} \mid$ / V	α
10	0.368	-0.770	0.136	0.386
20	0.568	-0.805	0.105	0.499
30	0.754	-0.832	0.080	0.656
40	0.981	-0.854	0.069	0.761
50	1.043	-0.870	0.068	0.772
Average				0.615

It can be seen from Fig. 5 (a) that peak potential E_p plotted vs. log v gives a linear response in the silver electroplating bath, which is characteristic to an irreversible electrode process for the silver electrodeposition.

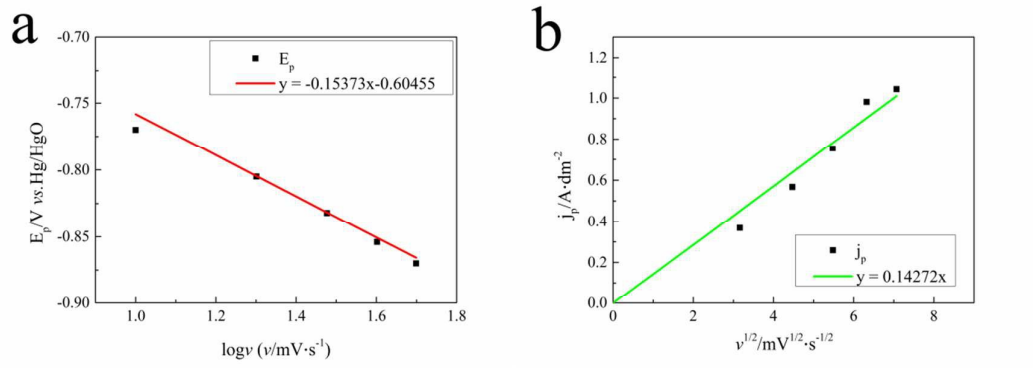

Fig. 5 (a) The peak potential (E_p) of CV with various sweep rates versus log v of the silver electroplating bath and (b) The peak current density (j_p) of CV with various sweep rates versus $v^{1/2}$ of the silver electroplating bath.

Fig. 5 (b) displayed that the j_p versus the square root of the scan rate ($v^{1/2}$) of the silver plating bath possess a linear response in the investigated silver plating bath, indicating that the discharge process of silver electrodeposition are diffusion

controlled in the silver electroplating bath. Which proves that silver electrodeposition in the studied bath is a typical irreversible process under diffusion control. The diffusion coefficient D in the silver plating bath containing 0.075 M Ag-complex was calculated to be 7.27×10^{-8} cm^2 s^{-1} from Fig. 5 (b) and Eq. (2).

3.4 Nucleation Mechanism

Early stages of the silver electrocrystallisation are important as they can determine the final morphology of the macroscopic and microcosmic structure of silver deposit, such as the brightness and smoothness. The nucleation rate and the number of crystallites formed can strongly depend on the overpotential. It is therefore important to establish the exact relationship between the overpotential and the nucleation rate as well as the number of crystallites. The classical electrochemical technique, chronoamperometry, is based on current transient measurements and has been extensively used to probe nucleation and growth phenomena in electrodeposition process. The chronoamperometry investigation of the silver plating bath in this work was displayed in Fig. 6.

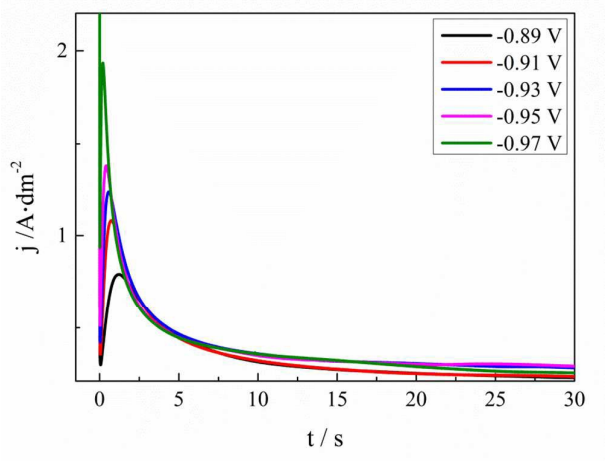

Fig. 6 Current transients at various applied potentials on the GCE of the DMH and NA based silver plating bath.

As shown in Fig. 6, all these *I*~*t* curves obtained from the DMH and NA based

silver plating bath have a common feature. At the very beginning of the potential step, the sharply current declines formed due to the double-layer charging. Then the current increases and reaches the maximum current peak at about 1.0 s to 2.0 s, and decrease subsequently after 2.0s because of the nucleation and the growth of the silver deposit and the variation of the diffusion layer. The Scharifer and Hills (SH)[43, 45, 46] model was employed to analyze the current transients measured in the present work. According to the SH models[33, 45, 47, 48] the relationship of current density (j) and time (t) can be expressed by, equation (3) and (4) for 3D instantaneous nucleation and progressive nucleation, respectively. All experimental current transients were transformed into non-dimensional curves of $(j/j_m)^2$ *vs* (t/t_m), and the curves were compared with theoretical current transients curves, as shown in Fig. 7.

$$(\frac{j}{j_m})^2 = 1.9542(\frac{t}{t_m})^{-1}\{1-\exp[-1.2564(\frac{t}{t_m})]\}^2 \quad (3)$$

$$(\frac{j}{j_m})^2 = 1.2254(\frac{t}{t_m})^{-1}\{1-\exp[-2.3367(\frac{t}{t_m})^2]\}^2 \quad (4)$$

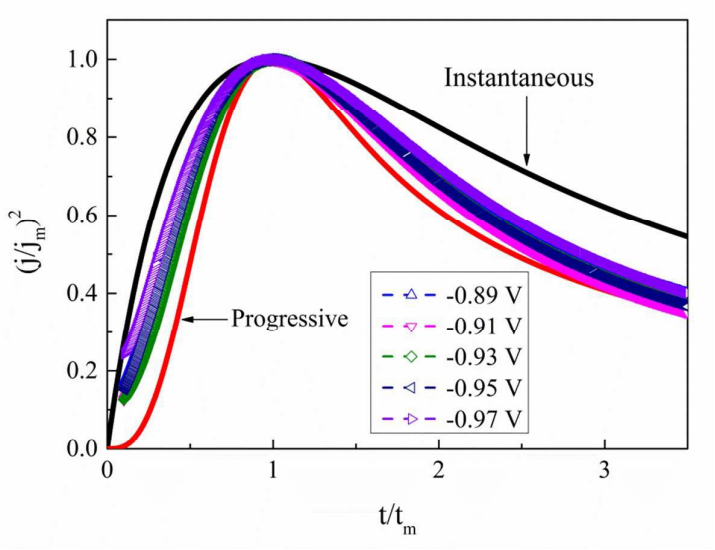

Fig. 7 Non-dimensional plots of instantaneous and progressive nucleation models with three-dimensional nuclei growth and experimental curves of the silver plating bath.

As displayed in Fig. 7, it is clear that the experimental curves of $(j/j_m)^2$ *vs* (t/t_m) at all potentials are very close to the theoretical curves of progressive nucleation. This indicates that the electrodeposition of silver on GCE from the electroplating bath have a progressive nucleation process.

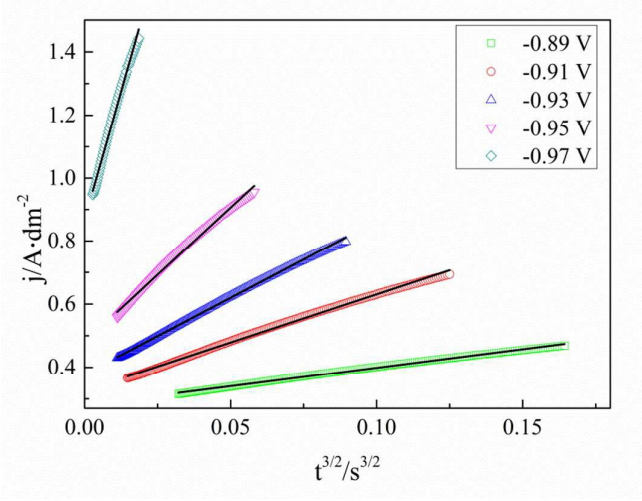

Fig. 8 Fits for the rising part of these transients to the progressive nucleation model of the silver plating bath.

For a 3D nucleation process, a linear relationship of *j vs.* t^x in the rising part of the current transients can be used to reveal the electrocrystallization mechanism. [29, 49] It is obviously that in our case, x = 3/2 makes *j vs.* t^x linear as displayed in Fig. 8. Therefore, it is reasonable that the silver electrocrystallization mechanism in this work is explained by 3D nucleation progressive model deduced from diffusion-controlled growth model, consisting well with the conclusions of CV measurement.

In the progressive nucleation process, equation (5) ~ (8) are always used for the study of diffusion coefficient, the nuclear number density, and nucleation rate constant.[22, 29, 45, 49-51]

$$t_m = \left(\frac{4.6733}{AN_\infty \pi K' D} \right)^{\frac{1}{2}} \quad (5)$$

$$j_m = 0.4615nFD^{\frac{3}{4}}c\left(AN_\infty K^{'}\right)^{\frac{1}{4}} \quad (6)$$

$$j_{\mathrm{m}}^2 t_{\mathrm{m}} = 0.2598(nFc)^2 D \quad (7)$$

$$K^{'} = \frac{4}{3}\left(\frac{8\pi cM}{\rho}\right)^{\frac{1}{2}} \quad (8)$$

Where A is a first order nucleation rate constant, N is the number density of nuclei, n is the number of electrons involved in the silver electro deposition reaction (n = 1), F is the Faraday constant, D is the diffusion coefficient, c is the concentration of electroactive species in the bath (c = 7.5×10 $^{-4}$ mol cm^{-3}), M is the molar mass and ρ is the density of the Ag deposit (M = 107.87 g mol $^{-1}$ and ρ = 10.5 g cm $^{-3}$).

The maximum value of the number of nuclei (saturation number N_s) and the vertical growth of silver nucleation (k_v) can be determined by equation (9)~ (11).

$$N_s = \left(\frac{AN_\infty}{2K^{'}D}\right)^{\frac{1}{2}} \quad (9)$$

$$AN_\infty = \frac{4.6733}{t_m{}^2 \pi K^{'} D} \quad (10)$$

$$k_{\mathrm{v}} = \frac{j_m}{nF} \quad (11)$$

Parameters according to Eq. (5)~(11) obtained from chronoamperometry at GCE in the studied cyanide-free silver plating bath with different applied potentials were summarized in Table 3.

As displayed in Table 3, the diffusion coefficient calculated using the data of *I-t* measurements was almost to the same as that from the CVs in Fig. 4 and Fig. 5.

Table 3 The parameters according to Eq. (5)~(11) obtained from chronoamperometry at GCE in the studied cyanide-free silver plating bath with different applied potentials.

E/V	j_m/A·dm^{-2}	t_m/s	D/10^{-8} cm^2 s^{-1}	AN_∞/10^8 cm^{-2} s	N_s/10^6 cm^{-2}	k_v/10^{-8} mol s^{-1} cm^{-2}
-0.89	0.792	1.198	5.522	0.320	7.030	8.207
-0.91	1.082	0.744	6.397	0.716	9.767	11.212
-0.93	1.236	0.569	6.387	1.227	12.796	12.808
-0.95	1.376	0.423	5.886	2.409	18.678	14.259
-0.97	1.935	0.202	5.557	11.189	41.429	20.052

It is observed that nucleation rate AN_∞ and saturation nuclei number N_s present an obvious increase with the applied potentials move negatively. Indicate that with a bigger overpotential, the nucleation rate can be expressed. The vertical growth of silver nucleation was significantly enhanced by the increase of the cathodic overpotential. As displayed in Fig. 9 and Fig. 10, lg k_v~E and ln N_s~E give linear responses in the investigated silver plating bath, proving that the growth of silver nucleation (k_v) and the nucleation rate of DMH and NA based silver plating bath were highly depended on the applied potential.

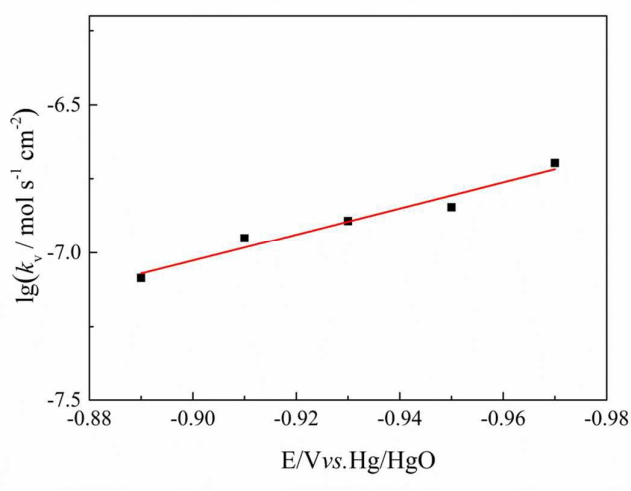

Fig. 9 lg k_v as a function of E for silver plating bath in DMH and NA based bath.

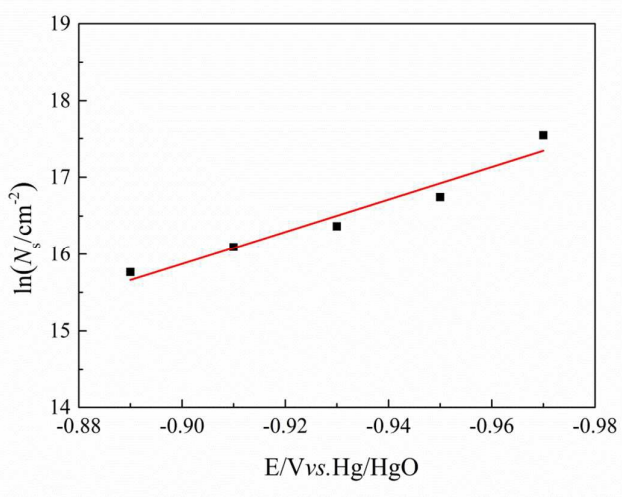

Fig. 10 ln N_s as a function of E for silver plating bath in DMH and NA based bath.

4. Conclusions

In the cyanide-free silver electroplating bath with DMH and NA as complexing agents, equally to the cyanide based silver electroplating bath, silver deposits with smooth and compact morphologies, as well as high purity could be obtained.

Based on the study of CV measurements, the deposition process of silver-complex in the DMH and NA based bath is irreversible. The transfer coefficient was calculated as 0.615 in the silver plating bath containing 0.075 M Ag-complex and the diffusion coefficient D in the silver plating bath was calculated to be 7.27×10^{-8} cm^2 s^{-1}. In the nucleation process study of the silver deposition, it is reasonable that the silver electrocrystallization mechanism in this work is explained by 3D nucleation progressive model. The diffusion coefficient calculated using the data of *I-t* measurements was almost similar to that from the CVs. It is observed that nucleation rate AN_∞ and saturation nuclei number N_s present an obvious increase with the applied potentials move negatively. The growth of silver nucleation (k_v) and the nucleation rate of silver deposit in DMH and NA based silver plating bath were highly depended

on the applied potential.

Acknowledgements

Financial support from the State Key Laboratory of Urban Water Resource and Environment (Harbin Institute of Technology) (2015DX09) for this work is gratefully acknowledged.

References

1. R. Zhang, W. Lin, K. Lawrence and C. P. Wong, *Int. J. Adhes. Adhes.*, 2010, **30**, 403-407.
2. Y. Shacham-Diamand, A. Inberg, Y. Sverdlov and N. Croitoru, *J. Electrochem. Soc.*, 2000, **147**, 3345-3349.
3. N. Fishelson, A. Inberg, N. Croitoru and Y. Shacham-Diamand, *Microelectron. Eng.*, 2012, **92**, 126-129.
4. R. Manepalli, F. Stepniak, S. A. Bidstrup-Allen and P. A. Kohl, *Advanced Packaging, IEEE Transactions on*, 1999, **22**, 4-8.
5. K. Márquez, G. Staikov and J. W. Schultze, *Electrochim. Acta*, 2003, **48**, 875-882.
6. B. C. Baker, M. Freeman, B. Melnick, D. Wheeler, D. Josell and T. P. Moffat, *J. Electrochem. Soc.*, 2003, **150**, C61-C66.
7. G. Baltrūnas, *Electrochim. Acta*, 2003, **48**, 3659-3664.
8. B. Bozzini, L. D'Urzo, C. Mele and V. Romanello, *J. Phys. Chem. C*, 2008, **112**, 6352-6358.
9. S. A. Hossain and M. Saitou, *J. Appl. Electrochem.*, 2008, **38**, 1653-1657.
10. R. Bomparola, S. Caporali, A. Lavacchi and U. Bardi, *Surf. Coat. Technol.*,

2007, **201**, 9485-9490.

11. Y. B. Patil and K. M. Paknikar, *Lett. Appl. Microbiol.*, 2000, **30**, 33-37.
12. C. L. Lasko and M. P. Hurst, *Environ. Sci. Technol.*, 1999, **33**, 3622-3626.
13. D. G. Foster, Y. Shapir and J. Jorne, *J. Electrochem. Soc.*, 2005, **152**, C462-C465.
14. D. G. Foster, Y. Shapir and J. Jorné, *J. Electrochem. Soc.*, 2003, **150**, C375-C380.
15. D. Gonnissen, S. Vandeputte, A. Hubin and J. Vereecken, *Electrochim. Acta*, 1996, **41**, 1051-1056.
16. S. Vandeputte, A. Hubin and J. Vereecken, *Electrochim. Acta*, 1997, **42**, 3429-3441.
17. B.-G. Xie, J.-J. Sun, Z.-B. Lin and G.-N. Chen, *J. Electrochem. Soc.*, 2009, **156**, D79-D83.
18. M. Miranda-Hernández and I. González, *J. Electrochem. Soc.*, 2004, **151**, C220-C228.
19. B. J. Polk, M. Bernard, J. J. Kasianowicz, M. Misakian and M. Gaitan, *J. Electrochem. Soc.*, 2004, **151**, C559-C566.
20. J.-C. Bian, Z. Li, Z.-D. Chen, H.-Y. He, X.-W. Zhang, X. Li and G.-R. Han, *Appl. Surf. Sci.*, 2011, **258**, 1831-1835.
21. G. M. Oliveira, M. R. Silva and I. A. Carlos, *J. Mater. Sci.*, 2007, **42**, 10164-10172.
22. Z.-B. Lin, B.-G. Xie, J.-S. Chen, J.-J. Sun and G.-N. Chen, *J. Electroanal. Chem.*, 2009, **633**, 207-211.
23. Z.-B. Lin, J.-H. Tian, B.-G. Xie, Y.-A. Tang, J.-J. Sun, G.-N. Chen, B. Ren, B.-W. Mao and Z.-Q. Tian, *J. Phys. Chem. C*, 2009, **113**, 9224-9229.

24. M.-C. Tsai, D.-X. Zhuang and P.-Y. Chen, *Electrochim. Acta*, 2010, **55**, 1019-1027.

25. A. Liu, X. Ren, M. An, J. Zhang, P. Yang, B. Wang, Y. Zhu and C. Wang, *Sci. Rep.*, 2014, **4**, 3837.

26. A. Liu, X. Ren, B. Wang, J. Zhang, P. Yang, J. Zhang and M. An, *RSC Adv.*, 2014, **4**, 40930-40940.

27. M. Puszyńska-Tuszkanow, T. Grabowski, M. Daszkiewicz, J. Wietrzyk, B. Filip, G. Maciejewska and M. Cieślak-Golonka, *J. Inorg. Biochem.*, 2011, **105**, 17-22.

28. A. Liu, X. Ren, J. Zhang, G. Yuan, P. Yang, J. Zhang and M. An, *New J. Chem.*, 2015, **39**, 2409-2412.

29. A. P. Abbott, M. Azam, G. Frisch, J. Hartley, K. S. Ryder and S. Saleem, *Physical Chemistry Chemical Physics*, 2013, **15**, 17314-17323.

30. G. M. de Oliveira, L. L. Barbosa, R. L. Broggi and I. A. Carlos, *J. Electroanal. Chem.*, 2005, **578**, 151-158.

31. G. M. de Oliveira, M. R. Silva and I. Carlos, *J. Mater. Sci.*, 2007, **42**, 10164-10172.

32. J. C. Ballesteros, E. Chaînet, P. Ozil, G. Trejo and Y. Meas, *J. Electroanal. Chem.*, 2010, **645**, 94-102.

33. F. Endres and W. Freyland, *J. Phys. Chem. B*, 1998, **102**, 10229-10233.

34. J. V. Zoval, R. M. Stiger, P. R. Biernacki and R. M. Penner, *The Journal of Physical Chemistry*, 1996, **100**, 837-844.

35. N. Hernández, J. M. Ortega, M. Choy and R. Ortiz, *J. Electroanal. Chem.*, 2001, **515**, 123-128.

36. J. M. Ortega, *Thin Solid Films*, 2000, **360**, 159-165.

37. J. P. Franey, G. W. Kammlott and T. E. Graedel, *Corros. Sci.*, 1985, **25**, 133-143.

38. C. Kleber, R. Wiesinger, J. Schnöller, U. Hilfrich, H. Hutter and M. Schreiner, *Corros. Sci.*, 2008, **50**, 1112-1121.

39. L. Paussa, L. Guzman, E. Marin, N. Isomaki and L. Fedrizzi, *Surf. Coat. Technol.*, 2011, **206**, 976-980.

40. S. Z. El Abedin, E. M. Moustafa, R. Hempelmann, H. Natter and F. Endres, *Electrochem Commun*, 2005, **7**, 1111-1116.

41. A. E. Alvarez and D. R. Salinas, *J. Electroanal. Chem.*, 2004, **566**, 393-400.

42. Y. Xiaowei, A. Maozhong, Z. Yunwang and Z. Lin, *Electrochim. Acta*, 2011, **58**, 516-522.

43. X. Ren, Y. Song, A. Liu, J. Zhang, P. Yang, J. Zhang, G. Yuan, M. An, H. Osgood and G. Wu, *RSC Adv.*, 2015, **5**, 64806-64813.

44. A. J. Bard and L. R. Faulkner, *Electrochemical Methods: Fundamentals and Applications*, Wiley, 2000.

45. B. Scharifker and G. Hills, *Electrochim. Acta*, 1983, **28**, 879-889.

46. M. E. Hyde and R. G. Compton, *J. Electroanal. Chem.*, 2003, **549**, 1-12.

47. A. I. Bhatt and A. M. Bond, *J. Electroanal. Chem.*, 2008, **619–620**, 1-10.

48. P. He, H. Liu, Z. Li, Y. Liu, X. Xu and J. Li, *Langmuir*, 2004, **20**, 10260-10267.

49. M. Miranda-Hernández, M. Palomar-Pardavé, N. Batina and I. González, *J. Electroanal. Chem.*, 1998, **443**, 81-93.

50. D. Gonnissen, W. Simons and A. Hubin, *J. Electroanal. Chem.*, 1997, **435**, 149-155.

51. Z. Zhang and D. P. Barkey, *J. Electrochem. Soc.*, 2007, **154**, D550-D556.

Table of contents

Silver deposit and electrochemical behaviors of silver-complex in the environmentally friendly silver plating bath were studied.